

# Development of a Microfluidics-based Flow Cytometer Using Disposable Lab-on-a-chip

Dae-Yun Lim<sup>1,\*</sup>, Tae Won Ha<sup>1,2,\*</sup>, and Chil-Hyoung Lee<sup>1,+</sup>

## Abstract

Fluorescence-activated cell sorting (FACS), which analyzes fluorescently stained cells in a flowing fluid and separates specific cell populations, is widely used across various fields, including molecular biology, pathology, and immunology. FACS has become an essential tool for advancing biotechnology. However, conventional flow cytometers have remained largely unchanged over the past 50 years, with improvements primarily limited to the addition of laser light sources and use of ultrasound to enhance accuracy. Conventional flow cytometers target only fluorescently labeled samples, necessitating complex modules to detect fluorescent signals and components to charge and separate target cells. Furthermore, they require calibration systems and mechanisms for cleaning flow channels and tubing when switching samples, adding to the instrument's structural complexity and cost. In this study, we designed a disposable microlab-on-a-chip system based on microelectromechanical systems to replace existing methodologies. By implementing hydrodynamic effects such as inertial focusing, inertial ordering, and Dean flow, we achieved particle alignment in a single direction. This led to the development of an innovative flow cytometry system that uses laser-induced light pressure to isolate specific cells.

**Keywords:** FACS, Disposable lab-on-a-chip, Flow cytometry system

## 1. INTRODUCTION

Conventional flow cytometers operate based on the principle of “hydrodynamic focusing,” where cells in a fluid stream are centered through laminar flow pressure, as described by Reynolds theory [1,2]. The core technology underpinning flow cytometry is particle alignment, which is achieved by constructing a microchannel, known as a flow channel, where a circular sheath fluid guides the sample fluid. This setup ensures that particles in the sample fluid are aligned and sequentially reach the detection area [3]. The flow cytometer was first commercialized by Becton, Dickinson and Company (US) and has become an integral part of life sciences research and diagnostics, benefiting from advances in associated devices and reagents. Although flow cytometers

provide rapid cellular physiology and biochemistry analyses, their fundamental design has remained largely unchanged over the last five decades, with improvements limited to increasing the number of laser light sources and incorporating ultrasound to improve accuracy.

Traditionally, flow channels are manufactured using femtosecond lasers or ultrafine machining technologies. However, because of the limitations of these techniques, issues such as burrs and inconsistent surface roughness arise, leading to unstable fluid flow and incomplete particle alignment in the sample fluid. Additionally, the sheath fluid required for measurement necessitates an expensive, ultraprecise fluid control system to manage two fluid types via complex algorithms, along with a cleaning system for channel maintenance. These requirements result in complex and costly equipment, while reducing measurement reliability. Owing to the high production costs associated with ultraprecise machining, conventional flow cytometers are cleaned and reused. This approach increases measurement time, operator fatigue, and the risk of cross-contamination and channel blockage. Currently, the domestic market for flow cytometers is dominated by three companies (Thermo Fisher, Becton Dickinson, and Beckman Coulter), presenting significant barriers for new domestic suppliers entering the market with conventional approaches [4].

<sup>1</sup>Energy & Nano Technology Group, Korea Institute of Industrial Technology (KITECH)

Gwangju 61012, Republic of Korea

<sup>2</sup>School of Materials Science & Engineering, Chonnam National University

Gwangju 61186, Republic of Korea

\*These authors are contributed equally to this work.

<sup>†</sup>Corresponding author: [chlee0901@kitech.re.kr](mailto:chlee0901@kitech.re.kr)

(Received : Nov. 5, 2024, Revised : Nov. 11, 2024, Accepted : Nov. 13, 2024)

This is an Open Access article distributed under the terms of the Creative Commons Attribution Non-Commercial License (<https://creativecommons.org/licenses/by-nc/3.0/>) which permits unrestricted non-commercial use, distribution, and reproduction in any medium, provided the original work is properly cited.

## 2. DEVELOPMENT OF MICROFLUIDICS-BASED LAB-ON-A-CHIP

### 2.1 Micropattern design

Microfluidics, distinct from general macroscopic fluid dynamics, applies microelectromechanical systems (MEMS) technology to create microscale channels. As shown in Fig. 1, the fluid motion in the microchannels displays a relatively predictable laminar flow. Particles flowing through these channels are automatically aligned in one direction because of inertial focusing, inertial ordering, and Dean flow [5,6].

Using these microfluidic properties, the flow channel was constructed to enable particle alignment without the sheath fluid required in conventional flow cytometers [7-9]. By employing the MEMS technology, various channel sizes can be customized to suit the measured particle sizes. As illustrated in Fig. 2, the designed lab-on-a-chip consists of two parts: the lower part containing the microchannel and inlet, and the upper part featuring

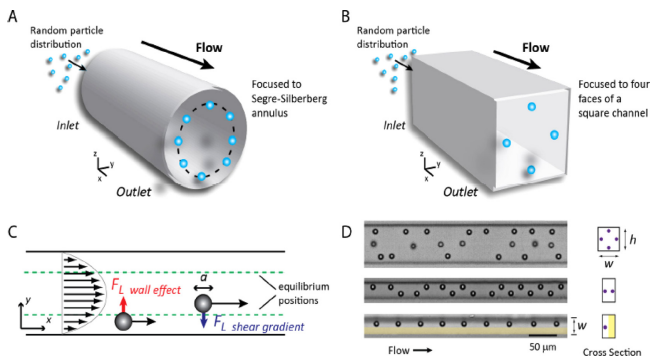


Fig. 1. Alignment effects of particles in microchannels based on microfluidics.

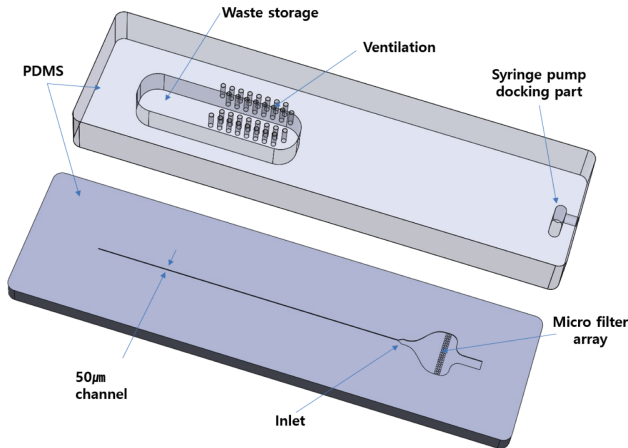


Fig. 2. Lab-on-a-chip design with 50 μm pattern.

the syringe pump docking and flow cell storage post-measurement.

The microchannel size was set to 50 μm, accommodating typical cell particle dimensions. Additional design features included a diverging channel to stabilize fluid flow and a microfilter array to remove foreign particles and lipids. The upper part incorporated ventilation to expel air, a docking area for syringe pump connection, and waste storage for flow cells after measurement. The entire system was constructed from polydimethylsiloxane (PDMS), with plasma bonding used to secure the top and bottom components.

### 2.2 Lab-on-a-chip fabrication using MEMS processes

In this study, microfluidic channels were designed and fabricated using lithography and dip-etching processes to achieve the desired channel linewidth. The primary goals were to precisely control the channel dimensions through photolithography and silicon dip etching and to create a fluid channel layout that ensures uniform sample injection.

The microfluidic channel was constructed by etching silicon

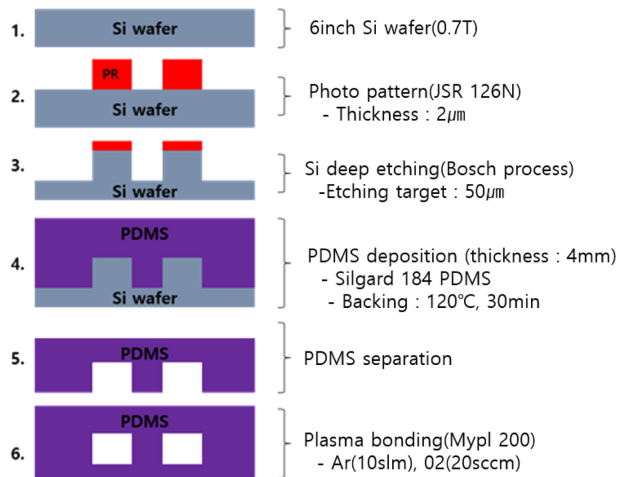


Fig. 3. MEMS process flowchart for lab-on-a-chip fabrication.

Table 1. Lab-on-a-chip fabrication conditions.

Etching condition (Bosch process)		Photo condition	
ICP/RF Power	1200/150 W	HMDS	110 °C, 60 sec
C4F8(5sec)	50 sccm	JSR Spin	1200 rpm, 30 sec
SF6(5sec)	100 sccm	Soft bake	90 °C, 300 sec
Pressure	8 mTorr	Exposure	10 sec
Chuck temp	7 °C	Develop	2 min
Run Time	600 cycle	Hard bake	110 °C, 240 sec

using MEMS processes, forming 50  $\mu\text{m}$  thick patterns based on the selectivity ratio between silicon and the etch mask material. The process conditions for achieving the desired channel dimensions and uniform etching are listed in Table 1.

### 2.3 Lab-on-a-chip measurement and analysis

The fabricated channels exhibit high precision and uniform cross-sectional profiles, ensuring reliable hydrodynamics in microfluidic applications such as particle alignment and separation. These results indicate that the designed processes satisfy the necessary specifications for precise microfluidic channel fabrication and fluid control. The geometries of the sample injection and filter portions of the microfluidic channels significantly affect fluid flow and sample alignment. After the silicon deep etching process, a 3D profiler and field emission scanning electron microscope (FE-SEM) were used to nondestructively measure the microstructures and evaluate the depth, geometry, and pattern consistency. This allowed us to compare the target and actual etch depths, thereby verifying the process quality and reliability.

The 3D profiler measured an average etch depth of 52.9  $\mu\text{m}$  (Fig. 4 (a)), while the FE-SEM obtained measurements of 48.59  $\mu\text{m}$  in width and 50.12  $\mu\text{m}$  in depth (Fig. 4 (b)). The profile angle was measured at  $89.1 \pm 1^\circ$ , indicating excellent accuracy. These analyses confirmed the shape and depth consistency of the micropattern structure after silicon deep etching, validating the reliability of the process.

### 2.4 Lab-on-a-chip plasma bonding

To fabricate a functional microchannel, bonding of the upper

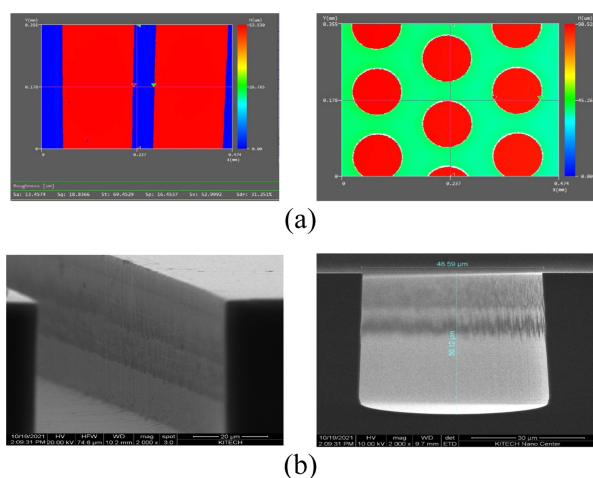


**Fig. 4.** Lab-on-a-chip measurement and analysis results of (a) 3D profiler and (b) FE-SEM.

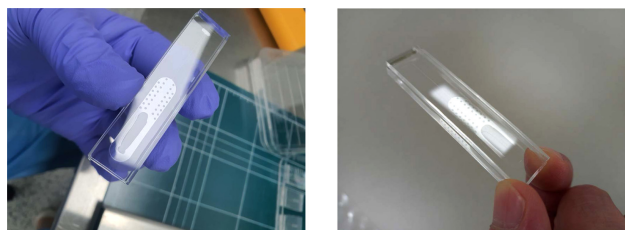


**Fig. 5.** Plasma-bonded lab-on-a-chip.

and lower structural components is essential. Traditional bonding methods are often insufficient owing to their small bonding areas. In this study, the PDMS underwent surface plasma treatment before bonding. This technique creates strong covalent bonds between the components, enabling the fabrication of a measurement kit containing a microchannel. The plasma bonding process utilized a MyPL\_200 atmospheric plasma system from APP Co., Ltd. Plasma treatment was applied to both PDMS surfaces, which were then bonded at the treated interfaces. Flow tests within the microchannel confirmed that this bonding method achieved the precision and stability required for effective microfluidic operation.

### 2.5 Fabrication of syringe-integrated lab-on-a-chip

For accurate diagnostics, reagents and samples should be delivered precisely, both quantitatively and at a stable flow rate, to designated locations. Variability and discontinuities in microfluidic delivery systems can considerably reduce the accuracy of results. Traditional syringe systems often encounter compatibility issues between the kit and syringe pump, requiring complex tubing and conduits. This complexity can lead to leakage and wastage of costly samples, which is particularly problematic in laboratory environments.

A design that integrates a syringe with a lab-on-a-chip is proposed, as illustrated in Fig. 6 (b). We eliminated the need for complex tubing and post-use cleaning protocols by utilizing PDMS to fabricate a disposable lab-on-a-chip. Moreover, using PDMS allows for high-precision micropatterning, enabling the creation of intricate channel designs essential for effective fluid control. Additionally, the plasma bonding process ensures that the integrated system can withstand high pressures while maintaining its integrity. This leads to minimal error rates in measurement data, thereby facilitating the acquisition of accurate and reliable diagnostic results. Thus, the syringe-integrated lab-on-a-chip not only simplifies the workflow but also enhances the performance and reliability of microfluidic applications in diagnostics.

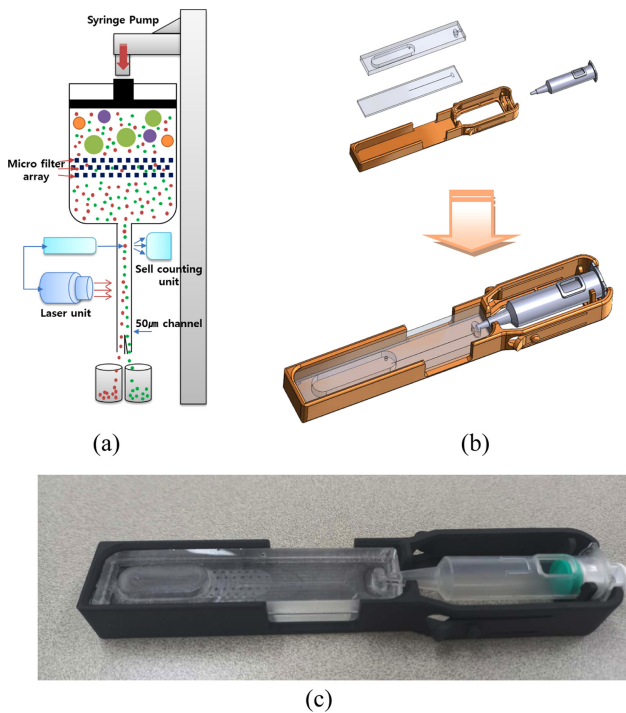


**Fig. 6.** Schematic of the flow cytometer and design of the syringe-integrated lab-on-a-chip: (a) Schematic of flow cytometer, (b) Design of syringe-integrated lab-on-a-chip, (c) Syringe-integrated lab-on-a-chip.

### 3. DEVELOPMENT OF AN OPTICAL SORTING MODULE

#### 3.1 Optical sorting module design

To enable cell sorting through laser-assisted optical pressure, an optical system was developed to align with the lab-on-a-chip architecture. This optical sorting system was engineered to facilitate efficient light trapping and achieve precise cell sorting within the microfluidic flow channel, as depicted in Fig. 7. A single-mode diode laser with a wavelength range of 650-1650 nm was used as the light source. The incident laser beam was focused using a high-magnification objective lens through a beam splitter. Various lenses were used to adjust the angle of incidence and laser power, optimizing the trapping conditions and achieving the ideal angle of incidence for effective cell sorting.

#### 3.2 Measuring the effect of phototrapping

In the experiment, 10  $\mu\text{m}$  and 20  $\mu\text{m}$  beads were used to simulate the cell flow in a conventional flow cytometer. The trapping performance was evaluated by varying parameters such as fluid velocity, laser wavelength, and angle of incidence. The

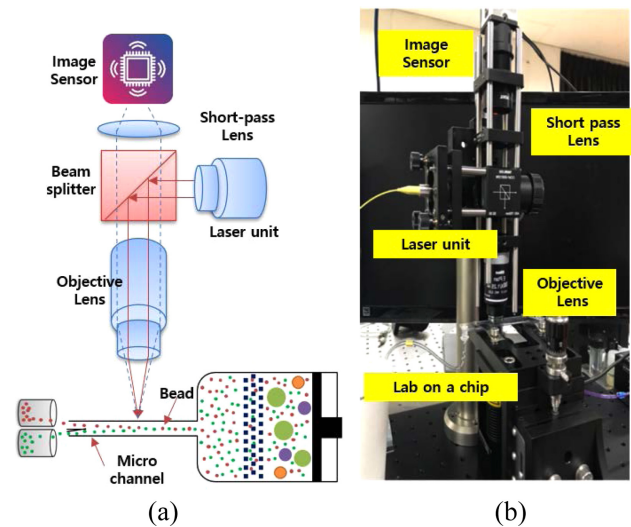


**Fig. 7.** Schematic and actual optical sorting system: (a) Schematic, (b) Actual system.

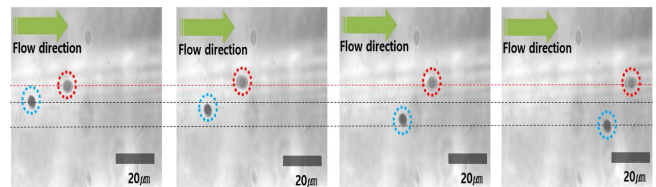


**Fig. 8.** Change in particle path due to phototrapping effects.

results indicated that an increase in the numerical aperture of the objective lens used for light trapping enhanced control over particle trajectories. Specifically, smaller particle sizes and higher refractive indices facilitated more precise manipulation of particle paths.

In the experiments, a laser power of approximately 12 mW was employed to achieve effective particle trapping at only 10% of the maximum power. This result demonstrated that similar trapping effects could be obtained using a relatively low-magnification objective lens.

The findings align with theoretical expectations: as the particle size increases, the required light intensity for effective trapping decreases. Furthermore, the trapping effect becomes more stable as the beam size and depth of focus increase. These results suggest that optimal trapping efficiency can be achieved by adjusting the parameters based on the particle size and specific optical conditions.

### 4. PROTOTYPING A FLOW CYTOMETER USING A DISPOSABLE LAB-ON-A-CHIP

#### 4.1 Mechanical design and prototyping



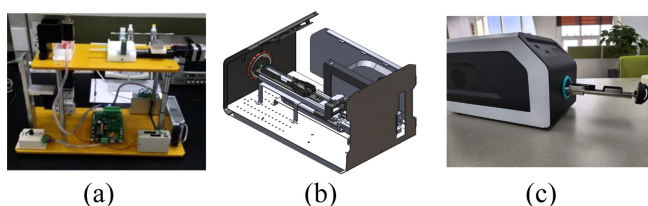


**Fig. 9.** Mechanical design and prototyping: (a) Test bed, (b) Mechanical design, (c) Prototype.

A disposable lab-on-a-chip cytometer prototype was developed by integrating a precision microfluidic delivery system with an optimized syringe mechanism. Several methodologies were implemented to satisfy the requirements for this design. As shown in Fig. 9 (a), a comprehensive algorithm was developed to ensure efficient operation of the syringe system. This algorithm manages key parameters, including pulse duration, operation time, and flow rate, which are essential for maintaining delivery accuracy across various experimental conditions and sample types. The microfluidic delivery system was engineered to accommodate a wide range of flow rates ranging from 200  $\mu\text{L/h}$  to 10,000  $\mu\text{L/h}$ , enabling flexibility to meet different experimental requirements and effectively process various sample types.

Miniaturization was prioritized in the design process to ensure compactness of the integrated system (Fig. 9 (b) and (c)). Advanced design principles and software modeling were employed to minimize the dimensions of the lab-on-a-chip and microfluidic components, while maintaining full functionality. A comprehensive mechanical design process was undertaken to ensure seamless integration of all system components. After the design phase, prototypes were produced to validate the design choices and functional performance of the system. Following successful verification of the performance of the microfluidic syringe system and related components, the focus shifted to product-oriented prototyping. This phase aimed to develop a reliable, high-performance microfluidic delivery system that meets the demands of cytometry applications. Through iterative testing and refinement, a robust system was developed, providing a strong foundation for further innovations in lab-on-a-chip technologies.

## 5. MEASUREMENT AND ANALYSIS

### 5.1 Cell separation and measurement by optical trapping effect

Optical sorting experiments were conducted within the flow

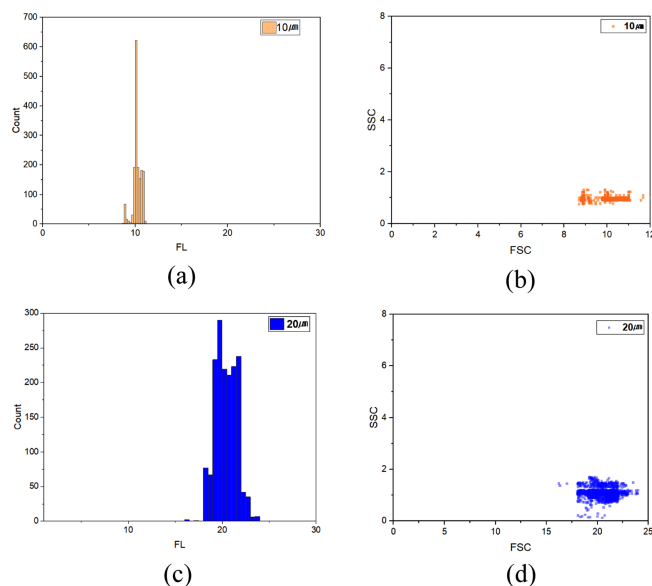


**Fig. 10.** Histograms and SSC/FSC charts for 10  $\mu\text{m}$  and 20  $\mu\text{m}$  beads: (a) 10  $\mu\text{m}$  histogram, (b) 10  $\mu\text{m}$  SSC/FSC charts, (c) 20  $\mu\text{m}$  histogram, (d) 20  $\mu\text{m}$  SSC/FSC charts.

channel to validate the performance of the optical sorter. The developed prototype cytometer consists of an FSC module, which measures forward-scattered light from particles, and an SSC module, which measures side-scattered light. By analyzing these two signals, the system can count the number and size of particles. The trigger signal for optical sorting was activated based on specific threshold values generated from the particle counting system. The light source intensity was adjusted to provide sufficient power for optical trapping, enabling selective sorting of particles. To verify the effect of optical trapping on cell sorting, polystyrene beads with diameters of 10  $\mu\text{m}$  and 20  $\mu\text{m}$  were used.

As shown in Fig. 10 (a), the measurements for the 10  $\mu\text{m}$  fluorescent beads range from 8 to 12  $\mu\text{m}$ , with a measurement error of less than 4%. This indicates a high level of reliability in cell size differentiation and cell counting. Additionally, Fig. 10 (b) illustrates the SSC/FSC chart for the 10  $\mu\text{m}$  beads, which further supports the observation that the measurements are primarily concentrated at approximately 10  $\mu\text{m}$ . Regarding the 20  $\mu\text{m}$  fluorescent beads, as depicted in Figs. 10 (c) and (d), the measurements range from 17 to 22  $\mu\text{m}$ , with an associated error rate of less than 5%. These findings confirm the accuracy of particle size differentiation and counting.

To further validate the effectiveness of the optical sorter, 10  $\mu\text{m}$  and 20  $\mu\text{m}$  beads were simultaneously flowed through the channel. As shown in Fig. 11, both bead sizes are successfully sorted. The observed error rate in this scenario is 8.7%, which is slightly higher than that recorded during sorting of a single bead

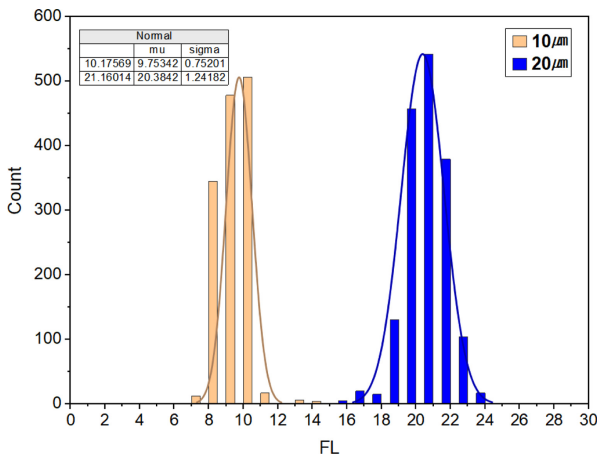


**Fig. 11.** Histograms of 10  $\mu\text{m}$  and 20  $\mu\text{m}$  beads flowing simultaneously.

type. This increase in error can be attributed to bead adhesion or overlap at elevated flow speeds within the microchannel, resulting in measurement inaccuracies.

## 6. CONCLUSIONS

The flow cytometer developed in this study achieves high precision and low measurement error through the application of MEMS technology. Additionally, it offers cost-effectiveness by utilizing a disposable lab-on-a-chip, which eliminates the need for a cleaning process. The introduction of a low-cost flow cytometer paired with a precise, disposable lab-on-a-chip that does not require cleaning minimizes exposure to contamination and biohazards between samples, addressing the inconvenience encountered by users who currently must clean the equipment after each use. Furthermore, this system presents opportunities for revenue generation through the sale of consumables. From a post-management perspective, this product addresses the challenges associated with existing equipment, which entail high maintenance costs and prolonged response times, thereby leveraging advancements in domestic technology. This approach is also effective in reducing overall management costs by establishing a domestic after-sales service system. With future advancements in technology and user interface simplification, this flow cytometer has the potential to evolve into a diagnostic device capable of providing a variety of diagnostic techniques. It is anticipated that

it could become an essential diagnostic tool utilized in clinical pathology departments. Through this commercialization strategy, the flow cytometer presented in this study is expected to transition from a laboratory-level analytical device to a diagnostic device suitable for hospital settings.

## ACKNOWLEDGMENT

This study was supported by KITECH (Project No. EO240003).

## REFERENCES

- [1] M. L. Shuler, R. Aris, and H. M. Tsuchiya, "Hydrodynamic focusing and electronic cell-sizing techniques", *Appl. Microbiol.*, Vol. 24, No. 3, pp. 384-388, 1972.
- [2] G. B. Lee, C. C. Chang, S. B. Huang, and R. J. Yang, "The Hydrodynamic Focusing Effect Inside Rectangular Microchannels", *J. Micromech. Microeng.*, Vol. 16, No. 5, pp. 1024-1032, 2006.
- [3] J. P. Robinson, J. Li, R. Ostafe, and S. N. Iyenga, "Flow Cytometry: The Next Revolution", *PMC PubMed Central*, Vol. 224, No. 2, pp. 281-290, 2023.
- [4] <https://www.marketresearchfuture.com/> - Flow Cytometry Market Size, Growth Analysis, Trends 2032 (retrieved on Nov. 4, 2024).
- [5] Q. Li, S. Cui, Y. Xu, Y. Wang, F. Jin, H. Si, L. Li, and B. Tang, "Consecutive Sorting and Phenotypic Counting of CTCs by an Optofluidic Flow Cytometer", *Anal. Chem.*, Vol. 91, No. 21, pp. 14133-14140, 2019.
- [6] Y. Zhang, B. R. Watts, T. Guo, Z. Zhang, C. Xu, and Q. Fang, "Optofluidic Device Based Microflow Cytometers for Particle/Cell Detection: A Review", *Micromachines*, Vol. 7, No. 4, p. 70, 2016.
- [7] D. Di Carlo, "Inertial Microfluidics", *Lab. Chip*, Vol. 9, No. 21, pp. 3038-3046, 2009.
- [8] J. Zhou and I. Papautsky, "Fundamentals of inertial focusing in microchannels", *Lab. Chip*, Vol. 13, No. 6, pp. 1121-1132, 2013.
- [9] T. Peng, J. Qiang, and S. Yuan, "Sheathless inertial particle focusing methods within microfluidic devices: a review", *Front. Bioeng. Biotechnol.*, Vol. 11, p. 1331968, 2018.
- [10] M. E. Piyasena and S. W. Graves, "The intersection of flow cytometry with microfluidics and microfabrication", *Lab. Chip*, Vol. 14, No. 6, pp. 1044-1059, 2014.
- [11] Y. Zhang, Y. Zhao, T. Cole, J. Zheng, J. Guo, and S. Y. Tang, "Microfluidic flow cytometry for blood-based biomarker analysis", *Analyst*, Vol. 147, No. 13, pp. 2895-2917, 2022.